

Random interface growth in random environment: Renormalization group analysis of a simple model

N. V. Antonov and P. I. Kakin

Department of Theoretical Physics, St. Petersburg University, Uljanovskaja 1,
St. Petersburg, Petrodvorez, 198504 Russia

E-mail: n.antonov@spbu.ru, p.kakin@spbu.ru

Abstract. We study effects of turbulent mixing on the random growth of an interface in the problem of the deposition of a substance on a substrate. The growth is modelled by the well-known Kardar–Parisi–Zhang model. The turbulent advecting velocity field is modelled by the Kraichnan’s rapid-change ensemble: Gaussian statistics with the correlation function $\langle vv \rangle \propto \delta(t - t') k^{-d-\xi}$, where k is the wave number and $0 < \xi < 2$ is a free parameter. Effects of compressibility of the fluid are studied. Using the field theoretic renormalization group we show that, depending on the relation between the exponent ξ and the spatial dimension d , the system reveals different types of large-scale, long-time asymptotic behaviour, associated with four possible fixed points of the renormalization group equations. In addition to known regimes (ordinary diffusion, ordinary growth process, and passively advected scalar field), existence of a new nonequilibrium universality class is established. Practical calculations of the fixed point coordinates, their regions of stability and critical dimensions are calculated to the first order of the double expansion in ξ and $\varepsilon = 2 - d$ (one-loop approximation). It turns out that for incompressible fluid, the most realistic values $\xi = 4/3$ or 2 and $d = 1$ or 2 correspond to the case of passive scalar field, when the nonlinearity of the KPZ model is irrelevant and the interface growth is completely determined by the turbulent transfer. If the compressibility becomes strong enough, the crossover in the critical behaviour occurs, and these values of d and ξ fall into the region of stability of the new regime, where the advection and the nonlinearity are both important. However, for this regime the coordinates of the fixed point lie in the unphysical region, so its physical interpretation remains an open problem.

PACS numbers: 05.10.Cc, 05.70.Fh

1. Introduction and description of the model

Over decades, constant interest has been attracted to the growth processes in various physical systems: solidification and flame fronts, smoke and colloid aggregates, tumors, and so on; see e.g. [1]–[9] and references therein. A most prominent example is provided by the deposition of a substance on a substrate and growth of the corresponding phase boundary (interface). A number of microscopic models were proposed to describe those phenomena: Eden model [6], Edwards–Wilkinson model [7], restricted solid-on-solid model [8], ballistic deposition [9]; not an exhaustive list.

It turns out, however, that the growth processes share some important features with those of equilibrium nearly-critical systems: namely, self-similar (scaling) behaviour (power-like dependencies) with rather universal (independent of the details of a specific process) exponents. In particular, the n -th order structure functions of a growth process behave as [1]–[5]

$$S_n(t, r) \equiv \langle [h(t, \mathbf{x}) - h(0, \mathbf{0})]^n \rangle \simeq r^{n\chi} F_n(tr^z), \quad r = |\mathbf{x}|. \quad (1.1)$$

Here $h(x) = h(t, \mathbf{x})$ is the height of the interface profile, the brackets $\langle \dots \rangle$ denote averaging over the statistical ensemble, χ and z are referred to as the roughness exponent and the dynamical exponent, respectively, and $F_n(\cdot)$ is a certain universal scaling function. The asymptotic behaviour (1.1) takes place in the infrared (IR) range, where the time and space differences t, r are large in comparison with characteristic microscopic scales.

It is then natural to try to describe universal properties of the growth processes on the base of a certain simplified model for a smoothed (coarse-grained) height field, in analogy with the theory of critical state, where most typical universality classes (types of critical behaviour) are described by the classical φ^4 -model [10, 11]. As the coarse-grained model of growth, one usually choses the Kardar–Parisi–Zhang (KPZ) model [12], described by the nonlinear stochastic differential equation

$$\partial_t h = \varkappa_0 \partial^2 h + \lambda_0 (\partial h)^2 / 2 + f. \quad (1.2)$$

Here the height field $h(x) = h(t, \mathbf{x})$ depends on the d -dimensional substrate coordinate \mathbf{x} , $\partial_t = \partial/\partial t$, $\partial_i = \partial/\partial x_i$, $\partial^2 = \partial_i \partial_i$ is the Laplace operator and $(\partial h)^2 = \partial_i h \partial_i h$; the summations over repeated tensor indices are always implied. The first term in the right-hand side of (1.2) describes the surface tension with the coefficient $\varkappa_0 > 0$. The second term represent an excess growth along the local normal to the surface. The parameter λ_0 can be of either sign; it can be scaled out, and in the following we set $\lambda_0 = 1$.

Furthermore, $f = f(x)$ is the Gaussian random noise with zero mean and given pair covariance

$$\langle f(x) f(x') \rangle = 2D_0 \delta(t - t') \delta^{(d)}(\mathbf{x} - \mathbf{x}'), \quad (1.3)$$

with the positive amplitude factor $D_0 > 0$.[‡]

To be precise, the model (1.2), (1.3) had appeared for the first time in the seminal paper by Forster, Nelson and Stephen [13] in terms of the purely longitudinal (solenoidal) vector field $u_i = \partial_i h$. Then, for $\lambda_0 = -1$ it represents the d -dimensional generalization of the Burgers equation. It can also be mapped onto a model of directed polymers in random media and on a model of Bose many-particle system with attraction; see e.g. [14].

Actually, the first two terms on the right-hand side of (1.2) are just the simplest local ones that respect the symmetries $h \rightarrow h + \text{const}$ and $O(d)$. Thus the KPZ model arises

[‡] Strictly speaking, a nonvanishing mean value $\langle f \rangle$ should be introduced in order to cancel a linear in-time growth of the mean value $\langle h \rangle$. Once we are interested in quantities like (1.1) that involve only differences of the fields, both the mean values can be simultaneously ignored.

ubiquitously in description of many nonequilibrium, disordered and driven diffusive systems. Then the field h can have different meanings. For example, in [15] the KPZ model and its ramifications were used to study large-scale distribution of matter in the Universe.

A few generalizations and modifications of the original KPZ model were introduced: random noise with finite correlation time [16], vector or matrix field h [17], modified form of the nonlinearity [18] and anisotropic modifications [19]. In connection to the latter, it is also worth to mention continuous anisotropic models of self-organized criticality [20].

The powerful quantitative theory of the critical state is provided by the field theoretic renormalization group (RG); see the monographs [10, 11] and references therein. In the RG approach, possible universality classes are associated with IR attractive fixed points of renormalizable field theoretic models.

The RG analysis of the KPZ model, pioneered in [13, 12], eventually (after some misunderstanding) led to the following conclusions [21], [23]. The field theoretic version of the stochastic problem (1.2)–(1.3) is multiplicatively renormalizable. The nonlinearity $(\partial h)^2$ in (1.2) is IR irrelevant (in the sense of Wilson) for $d > 2$, logarithmic (marginal) for $d = 2$ and relevant for $d < 2$. Thus it can be studied within the standard perturbative RG and the expansion in $\varepsilon \equiv 2 - d$. The corresponding RG equations possess a nontrivial fixed point with the exponents $\chi = 0$, $z = 2$ (the exact relation $\chi + z = 2$ is dictated by Galilean symmetry). However, the fixed point for $\varepsilon < 0$ is IR repulsive, while for $\varepsilon > 0$ it does not lie in the physical range of the model parameters ($D_0, \varkappa_0 > 0$) and thus can hardly describe the IR asymptotic behaviour of the problem. All these results are “perturbatively exact,” that is, exact in all orders of the expansion in ε .

One can nevertheless assume that the KPZ model possess a hypothetical IR attractive “strong-coupling” fixed point, not “visible” within any kind of perturbation theory. Then, for $d = 1$, the fluctuation-dissipation theorem along with the Galilean symmetry gives the exact values $\chi = 1/2$, $z = 3/2$ [12, 13]. With additional (rather nontrivial) assumptions, one derives definite exact values for the exponents in $d = 2$ and $d = 3$ [24]. Evidence of the existence of the strong-coupling point, provided by the so-called functional (also referred to as “exact” or “nonperturbative”) RG [25, 26], although convincing, is numerically still not too impressive, and the situation cannot be considered satisfactory; some other open problems are discussed e.g. in [27, 28].

It is well known that the behaviour of real systems near their critical points is very sensitive to external disturbances, gravity, finite-size effects, presence of impurities and so on; see e.g. [29, 30] for general discussion and references. What is more, some disturbances (randomly distributed impurities in magnets and turbulent mixing of fluid systems) can change the type of the phase transition or give rise to new universality classes with rich and rather exotic properties.

Investigation of the effects of various kinds of deterministic or chaotic flows (laminar shear flows, turbulent convection and so on) on the behaviour of the critical systems (like liquid crystals or binary mixtures near their consolution points) has shown that the flow can destroy the usual critical behaviour: it can change to the mean-field behaviour or,

under some conditions, to a more complex behaviour described by new non-equilibrium universality classes [31]–[37].

In this paper we study the influence of the random (turbulent) motion of the fluid, containing dissolved particles, on the IR behaviour of the randomly growing interface, paying special attention to the effects of compressibility. The advection by the velocity field $\mathbf{v}(x) \equiv \{v_i(x)\}$ is introduced by the “minimal” replacement

$$\partial_t h \rightarrow \nabla_t h \equiv \partial_t h + (v_i \partial_i) h, \quad (1.4)$$

where ∇_t is the Galilean covariant (Lagrangean) derivative.

We are going to acquire preliminary qualitative understanding of what can happen if the fluid motion is taken into account. For this reason, we neglect possible influence of the field $h(x)$ on the dynamics of the fluid (“passive” advection) and model the velocity field by simple Gaussian statistics with zero mean and prescribed pair covariance with vanishing correlation time:

$$\begin{aligned} \langle v_i(t, \mathbf{x}) v_j(t', \mathbf{x}') \rangle &= \delta(t - t') D_{ij}(\mathbf{x} - \mathbf{x}'), \\ D_{ij}(\mathbf{r}) &= B_0 \int_{k>m} \frac{d\mathbf{k}}{(2\pi)^d} \frac{1}{k^{d+\xi}} \{P_{ij}(\mathbf{k}) + \alpha Q_{ij}(\mathbf{k})\} \exp(i\mathbf{k} \cdot \mathbf{r}), \end{aligned} \quad (1.5)$$

known as the Kazantzev–Kraichnan ensemble; see e.g. [38]. Here $P_{ij}(\mathbf{k}) = \delta_{ij} - k_i k_j / k^2$ and $Q_{ij}(\mathbf{k}) = k_i k_j / k^2$ are the transverse and the longitudinal projectors, respectively, $k \equiv |\mathbf{k}|$ is the wave number, $B_0 > 0$ is an amplitude factor and $\alpha > 0$ is an arbitrary parameter. The case $\alpha = 0$ corresponds to the incompressible fluid ($\partial_i v_i = 0$), while the limit $\alpha \rightarrow \infty$ at fixed αB_0 corresponds to the purely potential velocity field. The exponent $0 < \xi < 2$ is a free parameter which can be viewed as a kind of Hölder exponent, which measures “roughness” of the velocity field; the “Kolmogorov” value is $\xi = 4/3$, while the “Batchelor” limit $\xi \rightarrow 2$ corresponds to smooth velocity. The cutoff in the integral (1.5) from below at $k = m$, where $m \equiv 1/\mathcal{L}$ is the reciprocal of the integral turbulence scale \mathcal{L} , provides IR regularization. Its precise form is unimportant; the sharp cutoff is the simplest choice for the practical calculations.

This ensemble, although it looks simple, has attracted enormous attention in turbulence studies because of the deep insight it offers into the origin of intermittency and anomalous multiscaling in turbulent advection and turbulence on the whole; see the review paper [38] and references therein. The RG approach to that problem is reviewed in [39]. In the context of our study, it is especially important that the Kazantzev–Kraichnan ensemble allows one to easily model compressibility, which appears rather difficult if the velocity field is described by Navier–Stokes equations; see e.g. [40, 41]. For a compressible fluid ($\partial_i v_i \neq 0$), the covariant derivative can also be introduced in an alternative way, namely, $\nabla_t h \equiv \partial_t h + \partial_i(v_i h)$, which is obligatory if the field h has the meaning of the density of some conserved quantity. In our case, however, h is “not conserved” due to the nonlinear term in (1.2), and in the following we will consider only the variant (1.4) because it preserves the symmetry $h \rightarrow h + \text{const}$ of the original KPZ problem.

The plan of the paper is the following. In section 2 we present the field theoretic formulation of the full stochastic problem (1.2), (1.3), (1.5) and diagrammatic technique. In section 3 we analyze ultraviolet (UV) divergences of the model and demonstrate its multiplicative renormalizability. Then the RG equations, as well as equations of critical scaling, can be derived in a standard way (section 4). The practical calculation of the renormalization constants and the RG functions is discussed in the Appendix. Fixed points of the RG equations and possible scaling regimes are studied in section 5. It turns out that, in addition to Gaussian fixed point (free field theory), purely “kinematic” regime (the KPZ nonlinearity is irrelevant in the sense of Wilson) and purely KPZ fixed point (turbulent transfer is irrelevant), the RG equations possess a fully nontrivial fixed point, in which both the nonlinearity and the mixing are important. The corresponding critical exponents can be calculated in the form of double expansions in ξ and $\varepsilon = 2 - d$; they are derived in the leading one-loop order.

The regions of IR stability of the fixed points in the parameter space ε , ξ and α are found. In particular it turns out, that for small α and most realistic values $d = 1$ or 2 and $\xi = 4/3$ or 2 , the IR asymptotic behaviour is governed by the kinematic fixed point with exactly known exponents. As the degree of compressibility α grows, the stability region of the full-scale point is getting wider and finally absorbs the realistic values of ε and ξ .

Derivation of the expressions like (1.1) requires (rather simple) analysis of the composite fields $h^n(x)$; this is discussed in section 6.

It should be admitted, however, that all of our practical results are derived within the framework of a standard “perturbative” field-theoretic RG. The strong-coupling IR attractive RG fixed point, if it indeed exists, definitely survives in the full-scale model, but the issue of its IR stability lies far beyond the scope of our study. This problem, along with some others, is discussed in sec. 7.

2. Field theoretic formulation of the model

Let us consider first the original KPZ model without the advection. According to the general statement [42] (see also the monographs [10, 11]), the stochastic problem (1.2), (1.3) is equivalent to the field theoretic model of the doubled set of fields $\Phi = \{h, h'\}$ with the action functional

$$\mathcal{S}(\Phi) = \frac{1}{2} h' D_0 h' + h' \left\{ -\partial_t h + \varkappa_0 \partial^2 h + \frac{1}{2} (\partial h)^2 \right\} \quad (2.1)$$

(we have set $\lambda_0 = 1$). Here and below, all needed integrations over $x = (t, \mathbf{x})$ and summations over repeated tensor indices are implied, e.g.,

$$h' D_0 h' = D_0 \int dt \int d\mathbf{x} h'(t, \mathbf{x}) h'(t, \mathbf{x}). \quad (2.2)$$

The field theoretic formulation means that various correlation functions and response functions of the stochastic problem (1.2), (1.3) can be identified with various Green functions of the field theoretic model with the action (2.1). In other words, they

are represented by functional averages over the full set of fields $\Phi = \{h, h'\}$ with the weight $\exp \mathcal{S}(\Phi)$.

The bare propagators in the corresponding Feynman diagrammatic techniques are determined by the free (bilinear in the fields) part of the action (2.1). In the frequency–momentum (ω – \mathbf{k}) representation they have the forms:

$$\begin{aligned} \langle hh' \rangle_0 &= \langle h'h \rangle_0^* = \frac{1}{-i\omega + \varkappa_0 k^2}, \\ \langle hh \rangle_0 &= \frac{D_0}{\omega^2 + \varkappa_0^2 k^4}, \quad \langle h'h' \rangle_0 = 0. \end{aligned} \quad (2.3)$$

The model has only one interaction vertex $h'(\partial h)^2/2$.

In the diagrammatic representation, we will denote $\langle hh \rangle_0$ as a straight line and $\langle hh' \rangle_0$ as a straight line with a small stroke that corresponds to the field h' .

Coupling with the velocity field $\mathbf{v}(x) \equiv \{v_i(x)\}$ is introduced by the substitution (1.4) in (1.2) and thus in (2.1). The full problem is then equivalent to the field theoretic model of the three fields $\Phi = \{h, h', \mathbf{v}\}$ with the action functional

$$\mathcal{S}(\Phi) = \frac{1}{2} h' D_0 h' + h' \left\{ -\nabla_t h + \varkappa_0 \partial^2 h + \frac{1}{2} (\partial h)^2 + f \right\} + \mathcal{S}_v. \quad (2.4)$$

The last term corresponds to the Gaussian averaging over the field \mathbf{v} with the correlator (1.5):

$$\mathcal{S}_v = -\frac{1}{2} \int dt \int d\mathbf{x} \int d\mathbf{x}' v_i(t, \mathbf{x}) D_{ij}^{-1}(\mathbf{x} - \mathbf{x}') v_j(t, \mathbf{x}'), \quad (2.5)$$

where D_{ij}^{-1} is the inverse to the integral operation D_{ij} from (1.5).

Thus the Feynman diagrams for the full model (2.4) involve, in addition to (2.3), the new propagator (1.5) and the new vertex $-h'(v\partial)h$.

The role of the coupling constants in the ordinary perturbation theory is played by the two parameters

$$g_0 = D_0/\varkappa_0^3 \sim \Lambda^\varepsilon, \quad w_0 = B_0/\varkappa_0 \sim \Lambda^\xi. \quad (2.6)$$

The last relations follow from the dimensionality considerations (see the next section) and define the typical UV momentum scale Λ .

3. UV divergences and renormalization

It is well known that the analysis of UV divergences is based on the analysis of the canonical dimensions (“power counting”); see, e.g., [10, 11]. The dynamic models of the type (2.4) have two independent scales: the time scale T and the length scale L (as opposed to single-scale static models).

Thus the canonical dimension of some quantity F (a field or a parameter in the action functional) can be completely described by two numbers, the frequency dimension d_F^ω and the momentum dimension d_F^k :

$$[F] \sim [T]^{-d_F^\omega} [L]^{-d_F^k}.$$

Table 1. Canonical dimensions of the fields and parameters in the model (2.4).

F	h	h'	v	\varkappa_0, \varkappa	D_0	g_0	B_0	w_0	g, w, α	m, μ, Λ
d_F^ω	1	-1	1	1	3	0	1	0	0	0
d_F^k	-2	$d+2$	-1	-2	$-d-4$	$2-d \equiv \varepsilon$	$-2+\xi$	ξ	0	1
d_F	0	d	1	0	ε	ε	ξ	ξ	0	1

They are found from the obvious normalization conditions

$$d_k^k = -d_{\mathbf{x}}^k = 1, \quad d_k^\omega = d_{\mathbf{x}}^\omega = 0, \quad d_\omega^k = d_t^k = 0, \quad d_\omega^\omega = -d_t^\omega = 1,$$

and from the requirement that each term of the action functional be dimensionless (with respect to the momentum and frequency dimensions separately). Then, based on d_F^k and d_F^ω , one can introduce the total canonical dimension $d_F = d_F^k + 2d_F^\omega$ (in the free theory, $\partial_t \propto \partial^2$). In the theory of renormalization of dynamical models this factor plays the same role as the conventional (momentum) dimension does in static problems; see Chap. 5 of [11].

Canonical dimensions of the fields and parameters in the model (2.4) are presented in table 1. It also includes renormalized parameters (the ones without the subscript “o”) and the renormalization mass μ that will be introduced later on.

From table 1 it follows the model is logarithmic at $d = 2$ and $\xi = 0$, when the both coupling constants g_0 and w_0 simultaneously become dimensionless. Hence, the UV divergences in the Green functions manifest themselves as poles in $\varepsilon = 2 - d$, ξ and, in general, in all their linear combinations.

The total canonical dimension of an arbitrary 1-irreducible Green function $\Gamma = \langle \Phi \cdots \Phi \rangle_{1\text{-ir}}$ with $\Phi = \{h, h', v\}$ in the frequency–momentum representation is given by the relation:

$$d_\Gamma = d + 2 - d_h N_h - d_{h'} N_{h'} - d_v N_v, \quad (3.1)$$

where $N_h, N_{h'}, N_v$ are the numbers of corresponding fields entering into the function Γ ; see, e.g., [11].

The total dimension d_Γ in the logarithmic theory (i.e., at $\varepsilon = \xi = 0$) is the formal index of the UV divergence: $\delta_\Gamma = d_\Gamma|_{\varepsilon=\xi=0}$. The superficial UV divergences, whose removal requires counterterms, can be present only in those functions Γ for which δ_Γ is a non-negative integer. The counterterm is a polynomial in frequencies and momenta of degree δ_Γ (provided the convention that $\omega \propto k^2$ is implied).

If, for some reason, a number of external momenta occurs as an overall factor in all diagrams of a certain Green function, the real index of divergence δ'_Γ will be smaller than δ_Γ by the corresponding number of unities. This is exactly what happens in our model: the field h enters the vertices $h'(\partial h)^2$ and $h'(v\partial)h$ only in the form of spatial derivatives. Thus any appearance of h in some function Γ gives such an external momentum, and the real index of divergence is given by the expression $\delta'_\Gamma = \delta_\Gamma - N_h$. Furthermore, h can appear in the corresponding counterterm only in the form of derivative.

From table 1 and the expression (3.1) one obtains:

$$\delta'_\Gamma = \delta_\Gamma - N_h = 4 - N_h - 2N_{h'} - N_v. \quad (3.2)$$

In dynamical models, all the 1-irreducible Green functions without the response fields vanish identically (their diagrams always involve closed circuits of retarded lines); see, e.g., [11]. The sample diagram is shown in Fig. 1. Thus in (3.2) it is sufficient to consider the case $N_{h'} > 0$.

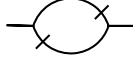


Figure 1. A diagram of the vanishing function $\langle hh \rangle_{1-ir}$ with a closed circuit of two retarded propagators.

Then straightforward analysis of the expression (3.2) shows that superficial UV divergences can be present only in the following 1-irreducible functions:

$$\begin{aligned} \langle h'h' \rangle_{1-ir} \quad (\delta_\Gamma = 0, \delta'_\Gamma = 0) & \quad \text{with the counterterm} \quad h'h', \\ \langle h'hh \rangle_{1-ir} \quad (\delta_\Gamma = 2, \delta'_\Gamma = 0) & \quad \text{with the counterterm} \quad h'(\partial h)^2, \\ \langle h'h \rangle_{1-ir} \quad (\delta_\Gamma = 2, \delta'_\Gamma = 1) & \quad \text{with the counterterm} \quad h'\partial^2 h, \\ \langle h'hv \rangle_{1-ir} \quad (\delta_\Gamma = 1, \delta'_\Gamma = 0) & \quad \text{with the counterterm} \quad h'(v\partial)h, \\ \langle h' \rangle_{1-ir} \quad (\delta_\Gamma = 2, \delta'_\Gamma = 2) & \quad \text{with the counterterm} \quad h', \\ \langle h'v \rangle_{1-ir} \quad (\delta_\Gamma = 1, \delta'_\Gamma = 1) & \quad \text{with the counterterm} \quad h'(\partial v), \\ \langle h'vv \rangle_{1-ir} \quad (\delta_\Gamma = 0, \delta'_\Gamma = 0) & \quad \text{with the counterterm} \quad h'v^2. \end{aligned} \quad (3.3)$$

Some additional considerations reduce the number of the counterterms.

The action of the KPZ model is invariant with respect to the transformation

$$h(t, \mathbf{x}) \rightarrow h(t, \mathbf{x} + \mathbf{u}t) - \mathbf{u} \cdot \mathbf{x}, \quad h'(t, \mathbf{x}) \rightarrow h'(t, \mathbf{x} + \mathbf{u}t) \quad (3.4)$$

with an arbitrary constant parameter \mathbf{u} . This invariance, which becomes the Galilean symmetry in terms of the vector field $\partial_i h$, is violated in the full model (2.1). However, the latter possesses another kind of the Galilean symmetry, namely,

$$\begin{aligned} h(t, \mathbf{x}) & \rightarrow h(t, \mathbf{x} + \mathbf{u}t), \quad h'(t, \mathbf{x}) \rightarrow h'(t, \mathbf{x} + \mathbf{u}t), \\ \mathbf{v}(t, \mathbf{x}) & \rightarrow \mathbf{v}(t, \mathbf{x} + \mathbf{u}t) - \mathbf{u} \end{aligned} \quad (3.5)$$

(it is important here that our velocity field is not correlated in time). This symmetry requires that the monomial $h'(v\partial)h$ enter the counterterms only in the form of invariant combination $h'\nabla_t h = h'\partial_t h + h'(v\partial)h$. The first term, however, is forbidden by the real index (3.2): the field h appears in it without the spatial derivative. Thus the second term is also forbidden (the cancellation of divergent terms from different diagrams can be checked in practical calculation, too). The Galilean symmetry also rules out the monomial $h'v^2$.

The counterterm $\propto h'$, stemming from the function $\langle h' \rangle_{1-ir}$, in terms of the original stochastic problem renormalizes the mean value of the random noise $\langle f \rangle$. This is

illustrated by the “tadpole” diagram in Fig. 2: it represents the one-loop contribution to the mean value $\langle \partial h \partial h \rangle$. As already mentioned (see the footnote on p. 2), these two mean values can simultaneously be ignored. In this respect, the contribution from $\langle h' \rangle_{1-ir}$ is similar to the shift of critical temperature in models of equilibrium critical behaviour.

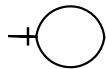


Figure 2. The one-loop “tadpole” diagram from the function $\langle h' \rangle_{1-ir}$.

The counterterm of the form $h' \partial_i v_i$, stemming from the Green function $\langle h' v \rangle_{1-ir}$, also requires special discussion. It vanishes identically for the incompressible case, where $\partial_i v_i = 0$. However, the practical one-loop calculation shows that it is absent in the general case ($\alpha \neq 0$). One can give some arguments that this is true in all orders of perturbation theory; see section Appendix A. Since our present analysis is restricted to the one-loop calculations, we will not take this term into account in the following discussion.

Then we are left with the three counterterms of the form $h'h'$, $h'\partial^2 h$ and $h'(\partial h)^2$. All these terms are present in the action (2.4) making our model multiplicatively renormalizable. The renormalized action then can be written in the form:

$$\mathcal{S}_R(\Phi) = \frac{1}{2} Z_1 h' D h' + h' \left\{ -\partial_t h + \varkappa Z_2 \partial^2 h + \frac{1}{2} Z_3 (\partial h)^2 + f \right\} + \mathcal{S}_v, \quad (3.6)$$

Here g , w and \varkappa are renormalized analogs of the bare parameters, and the functional \mathcal{S}_v from (2.5) should also be expressed in renormalized variables. The renormalization constants Z_i depend only on the completely dimensionless parameters g, w, \varkappa, α and absorb the poles in ε and ξ .

The renormalized action (3.6) is obtained from the original one (2.4) by the renormalization of the fields $h \rightarrow Z_h h$ and $h' \rightarrow Z_{h'} h'$ and of the parameters:

$$\varkappa_0 = \varkappa Z_\varkappa, \quad g_0 = g \mu^\varepsilon Z_g, \quad w_0 = w \mu^\xi Z_w. \quad (3.7)$$

The amplitudes D and B are expressed in renormalized parameters as follows:

$$D = g \varkappa^3 \mu^\varepsilon, \quad B = w \varkappa \mu^\xi. \quad (3.8)$$

The renormalization constants in Eqs. (3.6) and (3.7) are related as follows:

$$\begin{aligned} Z_g &= Z_1 Z_2^{-3} Z_3^2, & Z_\varkappa &= Z_2, & Z_h &= Z_3, & Z_{h'} &= Z_3^{-1}, \\ Z_h Z_{h'} &= 1, & Z_v &= 1, & Z_w Z_\varkappa &= 1. \end{aligned} \quad (3.9)$$

The first two relations in the second line follow from the absence of the counterterm $h' \nabla_t h$, the last relation follows from the absence of renormalization of the term \mathcal{S}_v .

The renormalization constants Z_1 – Z_3 are calculated directly from the diagrams, then the constants in (3.7) are found from (3.9). The renormalization constants can be found from the requirement that the Green functions of the renormalized model (3.6) be UV finite when expressed in renormalized variables. In our case this means that the

Green functions are UV finite at $\varepsilon, \xi \rightarrow 0$. The calculation in the first order in g and w (one-loop approximation) gives (see section Appendix A for the details):

$$Z_1 = 1 - \frac{1}{8\varepsilon}\hat{g} - \frac{\alpha}{2\xi}\hat{w}, \quad Z_2 = Z_3 = 1 - \frac{\hat{w}}{\xi} \frac{d-1+\alpha}{2d}, \quad (3.10)$$

where $\hat{g} = gS_d/(2\pi)^d$, $\hat{w} = wS_d/(2\pi)^d$, and $S_d = 2\pi^d/\Gamma(d/2)$ is the area of the unit sphere in d dimensions.

If the minimal subtraction (MS) scheme is employed, the renormalization constants must have the forms “ $Z = 1 +$ only poles in ε and ξ ” (and in higher orders in their linear combinations). Then, strictly speaking, in our one-loop accuracy we have to replace $d = 2 - \varepsilon \rightarrow 2$ in the above expressions. However, for some time we will keep them in the form (3.10): then some exact results for the special cases will be derived; see section 5. A similar renormalization scheme, where the dimension d is kept in “geometrical factors” stemming from contractions of various projectors, was earlier used in [21]; its validity and equivalence to the MS scheme was demonstrated in [22].

4. RG equations and RG functions

Consider briefly an elementary derivation of the RG equations; detailed exposition can be found in the monographs [10, 11]. The RG equations are written for the renormalized Green functions $G_R = \langle \Phi \cdots \Phi \rangle_R$. They differ from the original (unrenormalized) Green functions G by overall numerical factors (due to rescaling of the fields) and by different choice of the parameters (e, μ instead of e_0). Thus the renormalized Green functions can be equally used for analyzing the critical behaviour. The relation $S_R(Z_\Phi \Phi, e, \mu) = S(\Phi, e_0)$ between the functionals (2.4) and (3.6) yields the relations

$$G(e_0, \dots) = Z_h^{N_h} Z_{h'}^{N_{h'}} G_R(e, \mu, \dots). \quad (4.1)$$

between the Green functions. Here, as above, N_h and $N_{h'}$ are the numbers of corresponding fields entering into G (we take into account that in our model $Z_v = 1$); $e_0 = \{g_0, \varkappa_0, w_0\}$ is a full set of bare parameters and $e = \{g, \varkappa, w\}$ are their renormalized counterparts; the ellipsis stands for the other arguments (times, coordinates, momenta etc.).

We use $\tilde{\mathcal{D}}_\mu$ to denote the differential operation $\mu \partial_\mu|_{e_0}$. When expressed in the renormalized variables it looks as follows:

$$\mathcal{D}_{RG} \equiv \mathcal{D}_\mu + \beta_g \partial_g + \beta_w \partial_w - \gamma_\varkappa \mathcal{D}_\varkappa, \quad (4.2)$$

where $\mathcal{D}_x \equiv x \partial_x$ for any variable x . The anomalous dimensions γ are defined as

$$\gamma_F \equiv \tilde{\mathcal{D}}_\mu \ln Z_F \quad \text{for any quantity } F, \quad (4.3)$$

and the β functions for the two dimensionless couplings g and w are

$$\beta_g \equiv \tilde{\mathcal{D}}_\mu g = g[-\varepsilon - \gamma_g], \quad \beta_w \equiv \tilde{\mathcal{D}}_\mu w = w[-\xi - \gamma_w], \quad (4.4)$$

where the second equalities come from the definitions and the relations (3.7).

In order to derive the basic RG differential equations we apply to the both sides of the equality (4.1) the operation $\tilde{\mathcal{D}}_\mu$:

$$\{\mathcal{D}_{RG} + N_h\gamma_h + N_{h'}\gamma_{h'}\} G_R(e, \mu, \dots) = 0. \quad (4.5)$$

At last, equations (3.9) yield the following relations between the anomalous dimensions (4.3):

$$\begin{aligned} \gamma_h &= \gamma_3, & \gamma_{h'} &= -\gamma_3, & \gamma_w &= -\gamma_\varkappa, & \gamma_v &= 1, \\ \gamma_\varkappa &= \gamma_2, & \gamma_g &= \gamma_1 - 3\gamma_2 + 2\gamma_3. \end{aligned} \quad (4.6)$$

The anomalous dimension corresponding to a given renormalization constant Z_F can be found from the relation

$$\gamma_F = (\beta_g\partial_g + \beta_w\partial_w) \ln Z_F \simeq -(\varepsilon\mathcal{D}_g + \xi\mathcal{D}_w) \ln Z_F, \quad (4.7)$$

obtained from the definition (4.3), expression (4.2) for the operation $\tilde{\mathcal{D}}_\mu$ in renormalized variables, and the fact that the renormalization constants depend only on the two completely dimensionless coupling constants g and w . In the second part of the relation, we retained only the leading-order terms in the β functions (4.4) as it is sufficient for the first-order approximation. Utilizing the MS scheme, in the one-loop approximation from the explicit expressions (3.10) one finds:

$$\gamma_1 = \hat{g}/8 + \alpha\hat{w}/2, \quad \gamma_2 = \gamma_3 = \hat{w} \frac{d-1+\alpha}{2d}, \quad (4.8)$$

with \hat{g} and \hat{w} defined earlier (3.10) and the corrections of order \hat{g}^2 , \hat{w}^2 , $\hat{w}\hat{g}$ and higher.

5. Fixed points and scaling regimes

It is well known that the long-time large-distance asymptotic behaviour of a renormalizable field theory is determined by IR attractive fixed points of the corresponding RG equations. In general, the coordinates of possible fixed points are found from the requirement that all the β functions vanish. In the model (2.4) the coordinates g_* , w_* are determined by the two equations

$$\beta_g(g_*, w_*) = 0, \quad \beta_w(g_*, w_*) = 0, \quad (5.1)$$

with the β functions given in (4.4). The type of a fixed point is determined by the matrix

$$\Omega = \{\Omega_{ij} = \partial\beta_i/\partial g_j\}, \quad (5.2)$$

where β_i is the full set of the β functions and $g_j = \{g, w\}$ is the full set of coupling constants. For an IR attractive fixed point the matrix Ω should be positive, i.e., the real parts of all its eigenvalues should be positive.

From the relations (4.6) we find that $\gamma_g = \gamma_1 - \gamma_2$, $\gamma_w = -\gamma_\varkappa = \gamma_2$, so that

$$\begin{aligned} \beta_g &= g(-\varepsilon - \gamma_g) = g(-\varepsilon - \gamma_1 + \gamma_2), \\ \beta_w &= w(-\xi - \gamma_w) = w(-\xi - \gamma_2). \end{aligned} \quad (5.3)$$

Substituting explicit expressions (4.8) we arrive at the explicit one-loop expressions for the β functions:

$$\begin{aligned}\beta_g &= g \left\{ -\varepsilon - \frac{\hat{g}}{8} + \hat{w} \frac{(d-1)(\alpha-1)}{2d} \right\}, \\ \beta_w &= w \left\{ -\xi + \hat{w} \frac{(d-1+\alpha)}{2d} \right\},\end{aligned}\tag{5.4}$$

with possible corrections of the order w^2 and so on. It is worth noting that the one-loop result (5.4) for β_w becomes exact at $g = 0$ (see e.g. [39]), while the result for β_g becomes exact at $w = 0$ (as follows from the analysis of [23]).

From Eqs. (5.1) and (5.3) one finds that there are four different fixed points in our model. As $\partial_g \beta_w = 0$, the matrix Ω is triangular in every case and its eigenvalues are simply given by the diagonal elements $\Omega_g = \partial \beta_g / \partial g$ and $\Omega_w = \partial \beta_w / \partial w$.

The fixed points are as follows:

1. Gaussian (free) fixed point: $g_* = w_* = 0$; $\Omega_g = -\varepsilon$, $\Omega_w = -\xi$ (all these expressions are exact).
2. $w_* = 0$ (exact result to all orders), $\hat{g}_* = -8\varepsilon$; $\Omega_g = \varepsilon$, $\Omega_w = -\xi$.

This fixed points corresponds to pure KPZ model: although the interaction with the velocity field is present, it does not affect the leading-order IR asymptotic behaviour (it is irrelevant in the sense of Wilson).

3. $g_* = 0$ (exact), $\hat{w}_* = \frac{2d\xi}{(d-1+\alpha)}$; $\Omega_g = -\varepsilon + \xi - \frac{d\alpha\xi}{(d-1+\alpha)}$, $\Omega_w = \xi$ (exact).

This fixed points corresponds to pure Kraichnan model with small-scale stirring; the KPZ nonlinearity is irrelevant in the sense of Wilson.

4. $\hat{g}_* = 8 \left\{ -\varepsilon + \xi - \frac{d\alpha\xi}{(d-1+\alpha)} \right\}$, $\hat{w}_* = \frac{2d\xi}{(d-1+\alpha)}$; $\Omega_g = \varepsilon - \xi + \frac{d\alpha\xi}{(d-1+\alpha)}$, $\Omega_w = \xi$ (exact).

This fixed point corresponds to a new nontrivial IR scaling regime (universality class), in which the nonlinearity of the model (2.4) and the turbulent mixing are simultaneously important.

In figure 3 the regions of IR stability for all the fixed points in the ε - ξ plane are shown: dark space for the Gaussian point, horizontal shading for the KPZ point, vertical shading for the Kraichnan point and white space for the new regime. These regions are areas in which the eigenvalues of the matrix (5.2) for the given fixed point are both positive.

In the one-loop approximation (5.3), all the boundaries of the regions of stability are straight rays. Different regions have neither gaps nor overlaps between them. Such

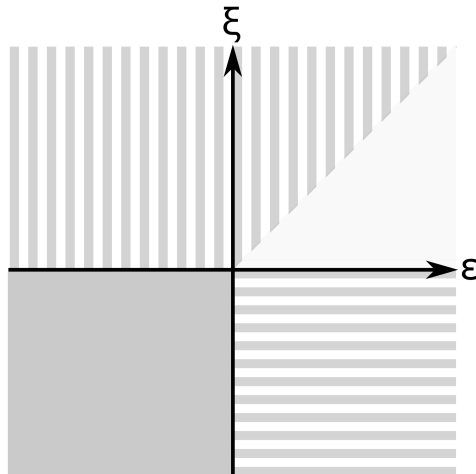


Figure 3. Regions of stability of the fixed points in the model (2.4).

a pattern is typical feature of the first-order approximations. The boundaries $\varepsilon < 0$, $\xi < 0$ for point 1, $\varepsilon > 0$ for point 2 and $\xi > 0$ for point 3 are exact, while the others can be affected by the higher-order corrections, i.e., the boundaries may become curved and gaps or overlaps may appear between the different regions of IR stability.

The main qualitative conclusion that can be drawn from this pattern, is that for small α and most realistic values $d = 1$ or 2 and $\xi = 4/3$ or 2 , the IR asymptotic behaviour is governed by the Kraichnan fixed point. However, as the degree of compressibility α increases, the stability region of the new point is getting wider and finally absorbs the realistic values of ε and ξ . Indeed, the boundary between the regions 3 and 4 depend on α . When α grows, it rotates counterclockwise and, for $\alpha \rightarrow \infty$, approaches the ray $\varepsilon = (1 - d)\xi$. Thus for $d = 1$ it tends to the vertical ray $\varepsilon = 0$, $\xi > 0$ and for $d = 2$ it tends to $\varepsilon = -\xi$, $\xi > 0$; see figure 4 (note, that for $d = 2$ the boundary becomes vertical at $\alpha = 1$).

We recall, however, that the results concerning the boundary between the regions 3 and 4 may be affected by the higher-order contributions. We also note that interpretation of the fixed point 4 leads to the same difficulty as that of the KPZ point: when it is IR attractive, the coordinate g_* lies in the unphysical region $g_* < 0$. We will return to this issue in section 7.

6. Critical dimensions. Critical scaling of the structure functions.

Composite fields $h^n(x)$.

Existence of an IR attractive fixed point implies existence of scaling (self-similar) behaviour of the Green functions in the IR range. In this critical scaling all the

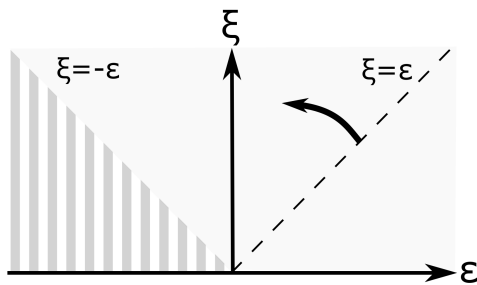


Figure 4. The boundary between the regions 3 and 4 moves counterclockwise with the growth of the compressibility α until it reaches the ray $\varepsilon = -\xi$ (for $d = 2$).

“IR irrelevant” parameters (μ , g and w in our case) are kept fixed, while the “IR relevant” parameters (coordinates/momenta, times/frequencies, the fields) are dilated. The critical dimension Δ_F of a certain IR relevant quantity F is given by the relations (with the normalization condition $\Delta_k = 1$)

$$\Delta_F = d_F^k + \Delta_\omega d_F^\omega + \gamma_F^*, \quad (6.1)$$

where

$$\Delta_\omega = 2 - \gamma_\varepsilon^* \quad (6.2)$$

is the critical dimension of frequency, $d_F^{k,\omega}$ are the canonical dimensions of F , given in table 1, and γ_F^* is the value of the anomalous dimension (4.3) at the fixed point in question: $\gamma_F^* = \gamma_F(g_*, w_*)$; see e.g. [11] for detailed explanation.

From table 1 for the dimensions of the fields we obtain

$$\Delta_h = -2 + \Delta_\omega + \gamma_h^*, \quad \Delta_{h'} = (d + 2) - \Delta_\omega + \gamma_h^*.$$

Then the relations (4.6) give

$$\Delta_\omega = 2 - \gamma_2^*, \quad \Delta_h = -\gamma_2^* + \gamma_3^*, \quad \Delta_{h'} = d + \gamma_2^* - \gamma_3^*.$$

Finally, substituting explicit one-loop expressions (4.8) yields

$$\Delta_h = 0, \quad \Delta_{h'} = d, \quad \Delta_\omega = 2 \quad (6.3)$$

for the fixed points 1 and 2 and

$$\Delta_h = 0, \quad \Delta_{h'} = d, \quad \Delta_\omega = 2 - \xi \quad (6.4)$$

for the points 3 and 4. For the points 1–3 these expressions are exact; see the remark below eq. (5.4). For the point 4 the dimensions of the fields can be affected by the higher-order contributions with the exact condition that $\Delta_h + \Delta_{h'} = d$, and the expression for Δ_ω is exact due to the second relation in (5.3).

In the traditional notation (1.1) one has $\Delta_h = -\chi$ and $\Delta_\omega = z$. However, the quantity S_n in (1.1) is not an ordinary n -th order Green function of the basic fields $h(x)$: it is a sum of pair correlation functions $\langle h^s(x)h^q(0) \rangle$ of the composite fields (“composite

operators” in the quantum-field terminology) $h^n(x)$. Renormalization of such quantities requires further analysis which, however, is rather simple in the present case.

Total canonical dimension of the 1-irreducible Green function $\Gamma = \langle F \Phi \dots \Phi \rangle_{1-ir}$ with one composite operator F and arbitrary number of basic fields $\Phi = \{h, h', v\}$ in our model is $d_\Gamma = d_F - d_h N_h - d_{h'} N_{h'} - d_v N_v$, where $N_h, N_{h'}, N_v$ are the numbers of corresponding fields entering into the function Γ , $d_{h,h',v}$ are their canonical dimensions and d_F is the canonical dimension of F ; see, e.g., [11]. The formal index of divergence is $\delta_\Gamma = d_\Gamma|_{\varepsilon=\xi=0}$; superficial divergences can be present in Γ if δ_Γ is a non-negative integer.

From table 1 for $F = h^n$ we obtain $d_F = 0$ and $\delta_\Gamma = -2N_{h'} - N_v$. Thus the divergences, at first sight, can be present in all functions $\Gamma = \langle h^n h \dots h \rangle_{1-ir}$ with $N_{h'} = N_v = 0$, arbitrary N_h and $\delta_\Gamma = 0$. However, any nontrivial diagram of such a function involves at least one external vertex $h'(\partial h)^2$ or $h'(v\partial)h$, where the field h stands under a derivative. Thus at least external momentum appears in the diagram as an overall factor, the real index δ'_Γ is negative and the superficial divergence is in fact absent.

This means that all the operators $F = h^n$ are not renormalized and their critical dimensions are simply given by $\Delta_F = n\Delta_h$. This justifies the relation (1.1) with the dimensions (6.3), (6.4).

7. Discussion and conclusion

We studied effects of turbulent mixing in the problem of randomly growing interface. The growth was modelled by the well-known Kardar–Parisi–Zhang stochastic equation (1.2), (1.3). The turbulent velocity field was modelled by the Kraichnan’s rapid-change ensemble (1.5).

The full problem can be reformulated as the multiplicatively renormalizable model with the action functional (2.4). Using the field theoretic RG we show that, depending on the relation between the exponent ξ and the spatial dimension d , the system exhibit different types of IR behaviour, associated with four possible fixed points of the RG equations. In addition to known regimes (ordinary diffusion, ordinary growth process, and passively advected scalar field), existence of a new nonequilibrium universality class is established.

Practical calculations of the fixed point coordinates, their regions of stability and critical dimensions were performed in the first order of the double expansion in ξ and $\varepsilon = 2 - d$ (one-loop approximation).

It was shown that for the incompressible fluid the most realistic values of ξ and d correspond to the universality class of passive scalar field, when the nonlinearity of the KPZ model is irrelevant. If the degree of compressibility α becomes large enough, the crossover in the IR behaviour occurs, and these values of d and ξ fall into the region of stability of the new regime.

However, a few problems remain open.

For the new universality class (as well as for the KPZ model) the coordinates

of the fixed point lie in the unphysical region $g_* < 0$, which corresponds to the “wrong” negative sign of the amplitude in the pair correlator (1.3). Thus it requires a careful physical interpretation. In this connection one can recall, that in the Doi–Peliti formalism [44, 45], where the original microscopic problem is formulated in terms of the creation-annihilation operators, the terms quadratic in the response fields can appear in the action functionals with the negative signs; see e.g. [45].

Another question is the fate of the strong-coupling fixed point of the pure KPZ model [25]. If it indeed exists, it definitely survives in our problem (with the second coordinate $w_* = 0$), but can become unstable. On the other hand, new nonperturbative fixed points with $w_* \neq 0$ can appear.

In our analysis we employed the simplest Kraichnan’s ensemble for the advecting velocity field. It would be interesting to consider more realistic models with non-Gaussianity, finite correlation time, anisotropy, etc. This work is in progress.

Acknowledgments

The authors are indebted to L.Ts. Adzhemyan for helpful discussion. The authors acknowledge Saint Petersburg State University for the research grant 11.38.185.2014.

Appendix A. Calculation of the renormalization constants

In this Appendix we shortly present derivation of the first-order results (3.10) for the renormalization constants. Although the one-loop calculation is rather simple and can be accomplished in a few different ways, it is worth to discuss it for completeness and in order to mention some interesting subtleties specific of the model (2.4).

The renormalization constants are determined by the requirement that the Green functions of the renormalized model (3.6), expressed in renormalized variables, be UV finite (in our case, be finite at $\varepsilon \rightarrow 0$, $\xi \rightarrow 0$). The full set of constants Z_1 – Z_3 can be found from the three 1-irreducible functions: $\langle h'h \rangle_{1\text{-ir}}$, $\langle h'h' \rangle_{1\text{-ir}}$ and $\langle h'hh \rangle_{1\text{-ir}}$. In the renormalized model, the corresponding one-loop approximations have the forms

$$\langle h'h \rangle_{1\text{-ir}} = i\eta - \varkappa p^2 Z_2 + \text{diagram 1} + \text{diagram 2}, \quad (\text{A.1})$$

$$\langle h'h' \rangle_{1\text{-ir}} = DZ_1 + \frac{1}{2} \text{diagram 3} + \text{diagram 4} \quad (\text{A.2})$$

and

$$\langle h'hh \rangle_{1\text{-ir}} = \text{diagram 5} + \text{diagram 6} + \text{diagram 7} + \text{diagram 8} + \dots$$

$$+ \quad + \quad + \quad . \tag{A.3}$$

Here we denoted the bare propagator $\langle hh \rangle_0$ as a straight line, $\langle hh' \rangle_0$ as a straight line with a small stroke that corresponds to the field h' , and the velocity propagator as the wavy line. In the following, we set the external frequency η equal to 0, because the divergent part of the function $\langle h' h \rangle_{1-\text{ir}}$ is proportional to p^2 , where p is the external momentum.

All the diagrammatic elements should be expressed in renormalized variables using the relations (3.6)–(3.9). In the one-loop approximation, the constants Z_i in the bare terms of (A.1), (A.2) and (A.3) should be taken in the first order in g and w , while in the one-loop contributions they should simply be replaced with unities, $Z_i \rightarrow 1$. Thus the passage to renormalized variables in the one-loop diagrams is achieved by the simple substitutions $\varkappa_0 \rightarrow \varkappa$, $g_0 \rightarrow g\mu^\varepsilon$ and $w_0 \rightarrow w\mu^\xi$.

The IR regularization in the diagrams involving the velocity propagator is provided by the cutoff in the integral (1.5) from below at $k = m$. In other diagrams, IR regularization is provided by external momenta and frequencies. We are interested, however, only in the UV divergent parts of these diagrams (poles in ε and ξ). Thus we will use the following trick, which simplifies the calculation: integrations over the momenta in all diagrams will be cut off from below at $k = m$. Then in the logarithmically divergent functions (A.2) and (A.3) external momenta and frequencies can be set equal to zero, when in the quadratically divergent function (A.1) we will keep only the p^2 term of the expansion in the external momentum p .

Now the integrations over the frequency are easily performed by residues. The resulting integrals over the momentum with the aid of the formulas

$$\int d\mathbf{k} k_i f(k) = 0, \quad \int d\mathbf{k} \frac{k_i k_s}{k^2} f(k) = \frac{\delta_{is}}{d} \int d\mathbf{k} f(k), \tag{A.4}$$

where $f(k)$ is any function depending only on $k = |\mathbf{k}|$, are reduced to the scalar integral

$$J(m) = \int_{k>m} d\mathbf{k} \frac{1}{k^{d+y}} = S_d \frac{m^{-y}}{y} \tag{A.5}$$

with S_d from (3.10). Here either $y = \varepsilon$ or $y = \xi$.

The last two diagrams in (A.3) in fact vanish and thus give no contribution to the renormalization constant. Indeed, they effectively involve closed circuits of retarded propagators; it is crucial here that the velocity correlator contains the δ function in time.

Direct calculation shows that the first three diagrams in (A.3) also give no contribution to Z_3 because their divergent parts cancel each other. This is a consequence of the Galilean symmetry (3.4) of the original KPZ model, which forbids the counterterm $h'(\partial h)^2$ in all orders of perturbation theory.

The analytic expression for the only remaining diagram in (A.3) has the form:

$$p_i p_j \int \frac{d\omega}{(2\pi)} \int_{k>m} \frac{d\mathbf{k}}{(2\pi)^d} \frac{k^2}{\omega^2 + \varkappa^2 k^4} \frac{w \varkappa \mu^\xi}{k^{d+\xi}} \{P_{ij}(\mathbf{k}) + \alpha Q_{ij}(\mathbf{k})\}. \quad (\text{A.6})$$

Here the prefactor comes from the two lower vertices, the first cofactor in the integrand comes from the upper vertex (numerator) and from the propagators $\langle h'h \rangle_0$ (denominator), and the remaining factor is the velocity correlator. Proceeding as explained above, we finally obtain for (A.3):

$$\langle h'h h \rangle_{1\text{-ir}} = p^2 \left\{ Z_3 + \frac{\hat{w}}{\xi} \left(\frac{\mu}{m} \right)^\xi \frac{(d-1+\alpha)}{2d} \right\}. \quad (\text{A.7})$$

The factor $(\mu/m)^\xi$ is UV finite: it tends to unity for $\xi \rightarrow 0$. We can see that, in order to cancel the pole in ξ in (A.7), the renormalization constant Z_3 can indeed be chosen in the form (3.10).

Now let us turn to the renormalization constant Z_2 .

The first one of the two diagrams in (A.1) appears UV finite and does not contribute to Z_2 . To see this, consider the corresponding analytic expression (up to insufficient amplitude factors):

$$\begin{aligned} & \int \frac{d\omega}{(2\pi)} \int_{k>m} \frac{d\mathbf{k}}{(2\pi)^d} \frac{k_i(p+k)_i k_j p_j}{\omega^2 + \varkappa^2 k^4} \frac{1}{-i\omega + \varkappa |\mathbf{k} + \mathbf{p}|^2} \propto \\ & \propto \int_{k>m} \frac{d\mathbf{k}}{(2\pi)^d} \frac{k_i(p+k)_i k_j p_j}{k^2(k^2 + |\mathbf{k} + \mathbf{p}|^2)}. \end{aligned} \quad (\text{A.8})$$

We are interested in the p^2 term of its expansion in p . It is a sum of two identical integrals with opposite signs. Indeed, the first one comes from the contribution $p_i p_j k_i k_j$ in the numerator; then in the denominator we can put $\mathbf{p} = 0$. The resulting integrand becomes equal to $p_i p_j k_i k_j / 2k^4$. The second one comes from the contribution $k_i k_i k_j p_j$. Then one has to expand the denominator up to the order $\mathcal{O}(\mathbf{p})$:

$$\int_{k>m} \frac{d\mathbf{k}}{(2\pi)^d} \frac{k_j p_j}{k^2 + |\mathbf{k} + \mathbf{p}|^2} \simeq \int_{k>m} \frac{d\mathbf{k}}{(2\pi)^d} \frac{k_j p_j}{2k^2} \left\{ 1 - \frac{(\mathbf{p}\mathbf{k})}{k^2} \right\}. \quad (\text{A.9})$$

The first term in (A.9) vanishes because the integrand is odd in \mathbf{k} , and the second equals to the aforementioned one up to the minus sign.

The analytic expression for the second diagram in (A.1) is as follows:

$$\int \frac{d\omega}{(2\pi)} \int_{k>m} \frac{d\mathbf{k}}{(2\pi)^d} \frac{i p_i i(p+k)_j}{k^{d+\xi}} w \varkappa \mu^\xi \frac{\{P_{ij}(\mathbf{k}) + \alpha Q_{ij}(\mathbf{k})\}}{-i\omega + \varkappa |\mathbf{k} + \mathbf{p}|^2}. \quad (\text{A.10})$$

Integration over ω involves the indeterminacy

$$\int \frac{d\omega}{(2\pi)} \frac{1}{-i\omega + \varkappa |\mathbf{k} + \mathbf{p}|^2} = \theta(0), \quad (\text{A.11})$$

where $\theta(0)$ is the Heaviside step function at the origin. This reflects the details of the velocity statistics lost in the white-noise limit; see the discussion in [38]. In the case at hand, the δ function in (1.5) should be understood as the limit of a narrow function which is necessarily *symmetric* in t, t' , because one deals with a pair correlator. Thus the indeterminacy in (A.11) must be unambiguously resolved as half the sum of the

limits: $\theta(0) = 1/2$. The integrand of the resulting integral over \mathbf{k} in (A.10) has an odd contribution that can be dropped and the even contribution that yields

$$\langle h'h \rangle_{1-ir} = -\varkappa p^2 \left\{ Z_2 + \frac{\hat{w}}{\xi} \left(\frac{\mu}{m} \right)^\xi \frac{(d-1+\alpha)}{2d} \right\}. \quad (\text{A.12})$$

We can see that Z_2 can be chosen in the form (3.10); in the one-loop approximation $Z_2 = Z_3$.

We will not discuss the calculation of Z_1 in detail: the first diagram reduces to the scalar integral (A.5) with $y = \varepsilon$ immediately after integration over the frequency. The analytic expression for the second diagram is similar to (A.6) with the replacement $p_i p_j \rightarrow k_i k_j$, so that only the contribution from the longitudinal projector survives. This leads to the replacement $(d-1+\alpha)/2d \rightarrow \alpha$. Bringing all contributions together and taking into account the symmetry coefficient $1/2$ for the first diagram, one obtains:

$$\langle h'h' \rangle_{1-ir} = D \left\{ Z_1 + \frac{1}{8} \frac{\hat{g}}{\varepsilon} \left(\frac{\mu}{m} \right)^\varepsilon + \alpha \frac{\hat{w}}{2\xi} \left(\frac{\mu}{m} \right)^\xi \right\}. \quad (\text{A.13})$$

We can see that the constant Z_1 that removes the poles from expression (A.13) can be taken in the form (3.10).



Figure A1. The one-loop contribution to the function $\langle h'v \rangle_{1-ir}$.

It remains to discuss possible UV divergence in the function $\langle h'v \rangle_{1-ir}$ with the counterterm $h' \partial_i v_i$. The only one-loop diagram for this function is shown in figure A1. It is not difficult to see that the corresponding analytical expression is nearly identical to that of the first diagram in the function (A.1): the latter only has additional extra factor p_j . Thus the diagram in question is also UV finite and does not give rise to the corresponding counterterm.

References

- [1] Krug J, Spohn H 1990 In: *Solids far from equilibrium. Ed. Godreche C* (Cambridge, Cambridge University Press)
- [2] Halpin-Healy T, Zhang Y-C 1995 *Phys. Rep.* **254** 215
- [3] Barabási A-L and Stanley H E 1995 *Fractal Concepts in Surface Growth* (Cambridge University Press)
- [4] Krug J 1997 *Adv. Phys.* **46** 139
- [5] Lässig M 1998 *Journ. Phys.: Condens. Matter.* **10** 9905
- [6] Eden M 1961 In: *Berkeley Symp. on Math. Statist. and Prob. Proc. Fourth Berkeley Symp. on Math. Statist. and Prob.* **4** 223 (Cambridge University Press)
- [7] Edwards S F and Wilkinson D R 1982 *Proc. R. Soc. London Ser. A* **381** 17
- [8] Kim J M, Kosterlitz J M and Ala-Nissila T 1991 *J. Phys. A: Math. Gen.* **24** 5569
- [9] Penrose M D 2008 *J. Stat. Phys.* **131** 247
- [10] Zinn-Justin J 1989 *Quantum Field Theory and Critical Phenomena* (Oxford: Clarendon)
- [11] Vasiliev A N 2004 *The Field Theoretic Renormalization Group in Critical Behavior Theory and Stochastic Dynamics* (Boca Raton, Chapman & Hall/CRC)

- [12] Kardar M, Parisi G and Zhang Y-C 1986 *Phys. Rev. Lett.* **56** 889
- [13] Forster D, Nelson D R and Stephen M J 1977 *Phys. Rev.* **16** 732
- [14] Kardar M and Zhang Y-C 1987 *Phys. Rev. Lett.* **58** 2087;
Bouchaud J P, Mézard M and Parisi G 1995 *Phys. Rev. E* **52** 3656;
Frey E, Täuber U C and Hwa T 1996 *Phys. Rev. E* **53** 4424
- [15] Pérez-Mercader J, Goldman T, Hochberg D and Laflamme R 1996 *Phys. Lett. A* **222** 177;
Barbero J F, Domínguez A, Goldman T. and Pérez-Mercader J 1997 *Europhys. Lett.* **38** 637;
Domínguez A, Hochberg D, Martín-García J M, Pérez-Mercader J and Schulman L S 1999
Astron. Astrophys. **349** 343;
Gaite J and Domínguez A 2007 *J. Phys. A: Math. Theor.* **40** 6849
- [16] Medina E, Hwa T, Kardar M and Zhang Y-C 1989 *Phys. Rev. A* **39** 3053;
Lam C-H and Sander L M 1992 *Phys. Rev. A* **46** R6128
- [17] Doherty J P, Moore M A, Kim J M and Bray A J 1994 *Phys. Rev. Lett.* **72** 2041;
Kardar M and Zee A 1996 *Nucl. Phys. B* **464** [FS] 449;
Bork L V and Ogarkov S L 2014 *Theor. Math. Phys.* **178** 359 [Translated from the Russian:
2014 *Teor. Mat. Fiz.* **178** 416]
- [18] Pavlik S I 1994 *JETP* **79** 303 [Translated from the Russian: 1994 *ZhETF* **106** 553];
Antonov N V and Vasil'ev A N 1995 *JETP* **81** 485 [Translated from the Russian: 1995 *ZhETF*
108 885]
- [19] Jeong H, Kahng B and Kim D 1996 *Phys. Rev. Lett.* **25** 5094
Kim H-J, Kim I-m and Kim J M 1998 *Phys. Rev. E* **58** 1144
- [20] Hwa T and Kardar M 1989 *Phys. Rev. Lett.* **62** 1813
Hwa T and Kardar M 1992 *Phys. Rev. A* **45** 7002
Tadić B 1998 *Phys. Rev. E* **58** 168
- [21] Frey E and Täuber U C 1994 *Phys. Rev. E* **50** 1024;
- [22] Wiese K J 1997 *Phys. Rev. E* **56** 5013
- [23] Lässig M 1995 *Nucl. Phys. B* **448** 559;
Wiese K J 1998 *J. Stat. Phys.* **93** 143
- [24] Lässig M 1998 *Phys. Rev. Lett.* **80** 2366
- [25] Canet L, Chaté H, Delamotte B and Wschebor N 2010 *Phys. Rev. Lett.* **104** 150601
- [26] Kloss T, Canet L and Wschebor N 2012 *Phys. Rev. E* **86** 051124
- [27] Lässig M and Kinzelbach H 1997 *Phys. Rev. Lett.* **78** 903
- [28] Hairer M 2013 *Ann. Math.* **178** 559
- [29] Ivanov D Yu 2008 *Critical Behaviour of Non-Ideal Systems* (Weinheim, Germany: Wiley-VCH)
- [30] Prudnikov V V, Prudnikov P V and Vakilov A N 2012 *Field-theoretic and Numerical Description
Methods for Critical Phenomena in Structure-Disordered Systems* (F.M. Dostoevsky University:
Omsk, Russia) [In Russian, English translation planned in: XXX]
- [31] Satten G and Ronis D 1985 *Phys. Rev. Lett.* **55** 91; 1986 *Phys. Rev. A* **33** 3415
- [32] Onuki A and Kawasaki K 1980 *Progr. Theor. Phys.* **63** 122;
Onuki A, Yamazaki K and Kawasaki K 1981 *Ann. Phys.* **131** 217;
Imaeda T, Onuki A and Kawasaki K 1984 *Progr. Theor. Phys.* **71** 16
- [33] Beysens D, Gbadamassi M and Boyer L 1979 *Phys. Rev. Lett* **43** 1253;
Beysens D and Gbadamassi M 1979 *J. Phys. Lett.* **40** L565
- [34] Ruiz R and Nelson D R 1981 *Phys. Rev. A* **23** 3224; **24** 2727;
Aronowitz A and Nelson D R 1984 *Phys. Rev. A* **29** 2012
- [35] Antonov N V, Hnatich M and Honkonen J 2006 *J. Phys. A: Math. Gen.* **39** 7867
- [36] Antonov N V and Ignatieva A A 2006 *J. Phys. A: Math. Gen.* **39** 13593
- [37] Antonov N V, Igloukov V I and Kapustin A S 2009 *J. Phys. A: Math. Theor.* **42** 135001
Antonov N V and Kapustin A S 2010 *J. Phys. A: Math. Theor.* **43** 405001
Antonov N V, Kapustin A S and Malyshev A V 2011 *Theor. Math. Phys.* **169** 1470 [Translated
from the Russian: 2011 *Teor. Mat. Fiz.* **169** 124]

- [38] Falkovich G, Gawędzki K and Vergassola M 2001 *Rev. Mod. Phys.* **73** 913
- [39] Antonov N V 2006 *J. Phys. A: Math. Gen.* **39** 7825
- [40] Volchenkov D Y and Nalimov M Y 1996 *Theor. Math. Phys.* **106** 307 [Translated from the Russian: 1996 *Teor. Mat. Fiz.* **106** 375];
Antonov N V, Nalimov M Y and Udalov A A 1997 *Theor. Math. Phys.* **110** 305 [Translated from the Russian: 1997 *Teor. Mat. Fiz.* **110** 385]
- [41] Antonov N V and Kostenko M M 2014 *Phys. Rev. E* **90** 063016
- [42] Martin P C, Siggia E D and Rose H A 1973 *Phys. Rev. A* **8** 423
- [43] De Dominicis C 1976 *J. Phys. (Paris) C* **1** 247;
Janssen H K 1976 *Z. Phys. B* **23** 377;
Bausch R, Janssen H K and Wagner H 1976 *Z. Phys. B* **24** 113;
- [44] Doi M 1976 *J. Phys. A* **9** 1479;
Grassberger P and Scheunert P 1980 *Fortschr. Phys.* **28** 547;
Peliti L 1984 *J. Phys. (Paris)* **46** 1469
- [45] Täuber U C 2002 *Acta Physica Slovaca* **52** 505; 2003 *Adv. Solid State Phys.* **43** 659;
2007 *Lect. Notes Phys.* **716** 295;
2009 In: *Encyclopedia of Complexity and System Science* Meyers R A (ed.) (Springer, New York) 3360 [*E-print LANL cond-mat/0707.0794*].